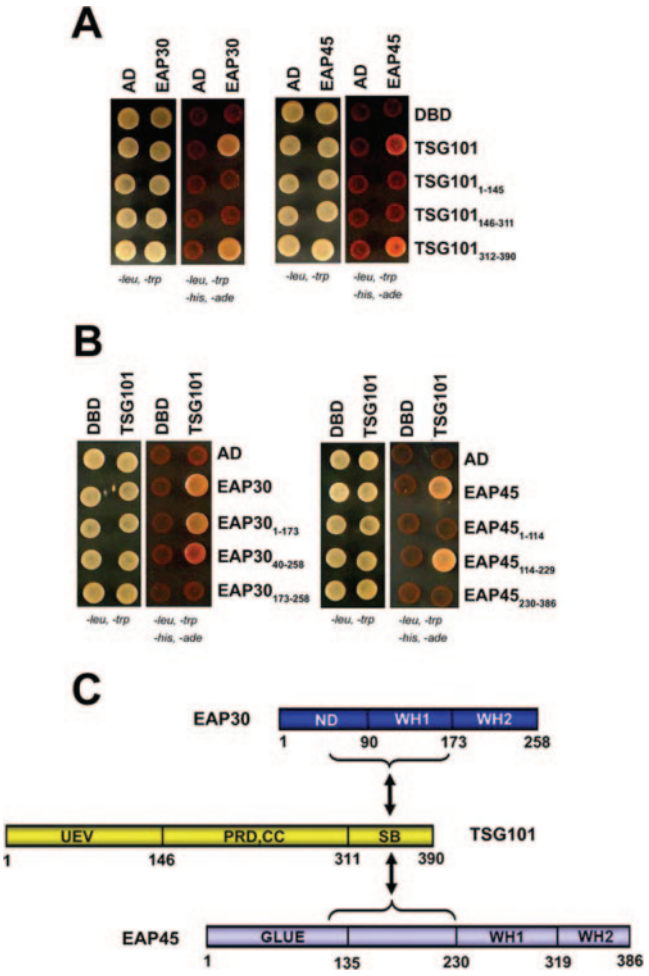

FIG. 2. Yeast two-hybrid mapping of the interaction sites between TSG101 and the EAP30 and EAP45 proteins. (A) Fragments of TSG101 binding to full-length EAP30 (left) and EAP45 (right). Selection media in the right and left arrays of each pair are the same as in Fig. 1C. (B) Full-length TSG101 binding to fragments of EAP45 (left) and EAP30 (right). (C) Schematic summary of fragment maps and interaction sites of TSG101, EAP30, and EAP45.

pected, however, and may have arisen because EAP30 was overexpressed in the absence of its other ESCRT-II binding partners. Alternatively, the interaction may reflect a natural tendency for ESCRT-II oligomerization (either directly or via bridging yeast proteins). In summary, all observed heteromeric intra-ESCRT-II interactions were consistent with structural models for the yeast and human ESCRT-II complexes, but the homomeric EAP30 interaction was not readily explained by the structure of isolated ESCRT-II.

ESCRT-I–ESCRT-II interactions. Two ESCRT-II proteins, EAP30 and EAP45, also interacted with TSG101, the central component of the ESCRT-I complex. Further mapping studies revealed that a fragment corresponding to the C-terminal region of TSG101 (termed the steadiness box [20, 42, 73]), was necessary and sufficient for both ESCRT-II protein interactions (Fig. 2A). Conversely, full-length TSG101 interacted with $EAP30_{1–173}$ and $EAP45_{114–229}$, but not with fragments outside of these regions (Fig. 2B). Thus, the TSG101 interaction site on EAP45 maps to the linker region between the GLUE domain and the first WH repeat. The TSG101 interaction site on EAP30 spans both the long N-terminal helical extension and the WH repeat. TSG101 also interacted, albeit less robustly, with an EAP30 fragment missing the first 40 amino acids that form the segment of the N-terminal helix that extends beyond the globular body of EAP30. Hence, the full EAP30 N-terminal helical extension is not strictly required for TSG101 binding, although this helix may contribute to the interaction, particularly as the full helix is predicted to extend to EAP30 residue 55.

As noted above, interactions between ESCRT-I and ESCRT-II must differ in the human and yeast systems, because the GLUE domain of human EAP45/ESCRT-II lacks the N-terminal NZF motif that forms the ESCRT-II interface in the yeast Vps28p/ESCRT-I–Vps36p/ESCRT-II complex (73). Nevertheless, we observed two-hybrid interactions for both EAP45/ESCRT-II and EAP30/ESCRT-II with human TSG101/ESCRT-I, indicating that the human ESCRT-I and ESCRT-II complexes can still interact, albeit via different ESCRT-I binding partners. Furthermore, the overall orientation of the ESCRT-I–ESCRT-II interaction may also be conserved, because the C-terminal region of TSG101 forms an extended interface with VPS28 (9, 42, 48, 73) and the TSG101 binding site on EAP45 lies immediately downstream (or at the very C-terminal end) of the GLUE domain. Thus, interactions between ESCRT-I and ESCRT-II appear to be retained in higher eukaryotes, although more detailed analyses of binding sites and energetics must await the production of pure recombinant human ESCRT complexes.

ESCRT-II–ESCRT-III interactions. In yeast, ESCRT-II recruits the downstream ESCRT-III complex through direct interactions between the ESCRT-II protein Vps25p (EAP20) and the ESCRT-III component Vps20p (CHMP6) (human homologs are in parentheses) (3, 74). Similarly, the human EAP20 and CHMP6 proteins also interacted in our two-hybrid survey of human class E proteins (Fig. 1C and 3A). Yeast two-hybrid mapping studies revealed that this interaction was mediated by the N-terminal half of CHMP6 binding to the C-terminal half of EAP20 (Fig. 3A), consistent with earlier reports (74, 88). The two C-terminal domains of EAP20 are exposed at the ends of the Y-shaped ESCRT-II complex, where they would be ideally positioned to nucleate ESCRT-III deposition through bivalent binding interactions (Fig. 1B).

GST pull-down and biosensor binding experiments with purified recombinant EAP20 and CHMP6 proteins demonstrated that the EAP20-CHMP6 interaction was direct, and these experiments again confirmed that EAP20 bound to the N-terminal half of CHMP6 (Fig. 3B and 4). As shown in Fig. 4A and B, the equilibrium binding isotherm for EAP20 binding to the full-length CHMP6 proteins fitted a simple 1:1 binding model with a dissociation constant of 5.3 $\pm$ 0.2 μM. Interestingly, EAP20 bound even more tightly to the N-terminal half of CHMP6 alone (residues 1 to 100) (equilibrium dissociation constant [K_D] = 601 $\pm$ 9 nM), and the increased affinity primarily reflected a significantly lower rate of EAP20 dissociation from the truncated CHMP6 fragment. This observation demonstrates that C-terminal sequences in CHMP6 reduce the EAP20 binding affinity, providing direct physical evidence for the proposal that isolated full-length ESCRT-III proteins can